

Article

Exploring the Diversity of Nuclear Density through Information Entropy

Wei-Hu Ma ^{1,2} and Yu-Gang Ma ^{1,2,*} 

¹ Key Laboratory of Nuclear Physics and Ion-beam Application (MOE), Institute of Modern Physics, Fudan University, Shanghai 200433, China; mawei@fudan.edu.cn

² Shanghai Research Center for Theoretical Nuclear Physics, NSFC and Fudan University, Shanghai 200438, China

* Correspondence: mayugang@fudan.edu.cn

Abstract: This study explores the role of information entropy in understanding nuclear density distributions, including both stable configurations and non-traditional structures such as neutron halos and α -clustering. By quantifying the uncertainty and disorder inherent in nucleon distributions in nuclear many-body systems, information entropy provides a macroscopic measure of the physical properties of the system. A more dispersed and disordered density distribution results in a higher value of information entropy. This intrinsic relationship between information entropy and system complexity allows us to quantify uncertainty and disorder in nuclear structures by analyzing various geometric parameters such as nuclear radius, diffuseness, neutron skin, and cluster structural features.

Keywords: information entropy; nuclear density distribution; halo nuclei; nuclear clustering

1. Introduction

Information entropy, a concept introduced by Claude Shannon to measure uncertainty in communication theory [1], has extensive applications in many scientific disciplines. In nuclear physics, a pioneering study on information entropy was performed in Ref. [2], where the multiplicity information was proposed and applied to search for nuclear liquid gas phase transition [3,4]. Applications of entropy or information entropy have been extended in different physics fields, e.g., Refs. [5–17]. It has become a valuable tool for the study of complex systems, providing a way to quantify uncertainty and disorder in nuclear systems. Its applications range from the study of nuclear structure to the analysis of the dynamics of particle production in high-energy collisions [18–21]. As the field advances, the integration of information entropy with theoretical models and experimental data could lead to deeper insights into the fundamental properties of nuclear matter.

Research on weakly bound nuclei has revealed unique quantum phenomena such as halo and skin formation [22–35], molecular orbitals, and cluster structures [36–46]. These discoveries have reshaped our understanding of nucleon distributions in atomic nuclei, which often deviate from idealized spherical or geometric models. The resulting patterns are complex and irregular, driven by factors such as nucleon interactions, energy levels, and clustering dynamics.

These non-uniform nucleon distributions result in regions of varying density, from densely packed areas to sparser edges. This irregularity directly affects the strength and range of nuclear forces, which, in turn, affects how nuclei interact and behave during reactions [47,48]. This complexity challenges traditional models of nuclear structure and underscores the need for more nuanced investigations.

Understanding these dynamics is critical to accurately modeling nuclear structures and predicting their behavior in various situations. By studying these patterns, researchers can gain deeper insights into the coexistence of mean-field and cluster dynamics, shedding light on fundamental nuclear properties and processes. This knowledge is central to

arXiv:2409.19260v1 [nucl-th] 28 Sep 2024



Citation: Ma, W.H.; Ma, Y.G.
Exploring the Diversity of Nuclear
Density through Information Entropy.
Entropy **2024**, *1*, 0. <https://doi.org/>

Academic Editor: Firstname
Lastname

Received: 25 July 2024

Revised: 28 August 2024

Accepted: 3 September 2024

Published:



Copyright: © 2024 by the authors.
Licensee MDPI, Basel, Switzerland.
This article is an open access article
distributed under the terms and
conditions of the Creative Commons
Attribution (CC BY) license (<https://creativecommons.org/licenses/by/4.0/>).

the advancement of nuclear physics and can guide future studies of nuclear interactions and reactions.

In analogy to the information entropy for discrete values, the differential entropy for a continuous random variable X with probability density function $f(x)$ is defined [49] as

$$S(X) = - \int_X f(x) \ln f(x) dx, \quad (1)$$

with the normalization condition $\int_X f(x) dx = 1$. This approach supports the broader application of information entropy in nuclear physics, allowing the analysis of continuous distributions.

The purpose of this study is to explore how information entropy is used in nuclear physics to understand nuclear density distributions, including both stable configurations and unconventional arrangements such as the halo structure and the α clustering structure. The total information entropy of a system can serve as a comprehensive measure of physical information, providing a view of the nucleon distribution in a nuclear many-body system that reflects the disordered information of spatial configurations.

2. Information Entropy of Diverse Nuclear Structures

2.1. Information Entropy of the Density Distribution with Woods–Saxon Type

The nuclear Woods–Saxon distribution is a widely used model in nuclear physics to describe the spatial distribution of nucleons in an atomic nucleus [50–53]. It is essential for the study of heavier nuclei with diffuse surfaces and provides a smooth transition from the high-density core to the low-density edge, accurately reflecting the structure of many nuclei. Its flexibility allows it to fit experimental data, making it a valuable tool in nuclear physics for analyzing structures and processes such as reactions, scattering, and decay.

The nuclei ^{16}O , ^{40}Ca , ^{116}Sn , and ^{208}Pb with Woods–Saxon type density distribution [52]

$$\rho(r) = \frac{\rho_0}{1 + e^{(r-R_0)/a}} \quad (2)$$

are considered as examples to examine the information entropy. The normalization coefficient ρ_0 , the diffuseness parameter a , and the radius R_0 satisfy the normalization condition

$$\int_0^\infty \frac{4\pi\rho(r)r^2}{W} dr = 1 \quad (3)$$

where W can be the number of protons Z , neutrons N , or nucleons $A = N + Z$. The parameters R_0 and a describe the spatial distribution of protons and neutrons in a nucleus. The R_0 parameter for proton and neutron distributions is denoted as R_{0p} and R_{0n} , respectively [52]. They are given by $R_{0p} = 1.81Z^{1/3} - 1.12$ and $R_{0n} = 1.49N^{1/3} - 0.79$. The a parameter for the proton and neutron distributions is defined as $a_p = 0.47 - 0.00083Z$ and $a_n = 0.47 + 0.00046N$, respectively. The diffuseness parameters a_p and a_n of the nuclei ^{16}O , ^{40}Ca , ^{116}Sn , and ^{208}Pb are scaled by the same parameter n_a to serve as a variable. The diffuseness parameters are modified by the scaling factor n_a , which serves as a variable to adjust the diffuseness parameters and, consequently, alter the density distribution. By using Equation (4), we can calculate the entropy as a function of n_a and analyze the correlation between entropy and the diffuseness parameter.

The information entropy in the nuclear system with radial density distribution of the Woods–Saxon type is defined as

$$S/k_B = - \int_0^\infty \frac{4\pi\rho(r)r^2}{W} \ln \frac{4\pi\rho(r)r^2}{W} dr, \quad (4)$$

where k_B is the Boltzmann constant, introduced to maintain the consistency of units in information entropy, rather than to highlight its thermodynamic significance. As shown in Figure 1, the information entropy tends to increase linearly with an increasing diffusion

parameter, indicating an increase in the uncertainty of the radial distribution of nucleons. Heavier nuclei exhibit larger information entropy values, suggesting that a greater number of nucleons enhances the complexity of the nuclear distribution and increases the uncertainty in the nuclear radial distribution. However, the rate of increase in information entropy for heavier nuclei is less pronounced, indicating a potential saturation effect as the system reaches a certain level of complexity.

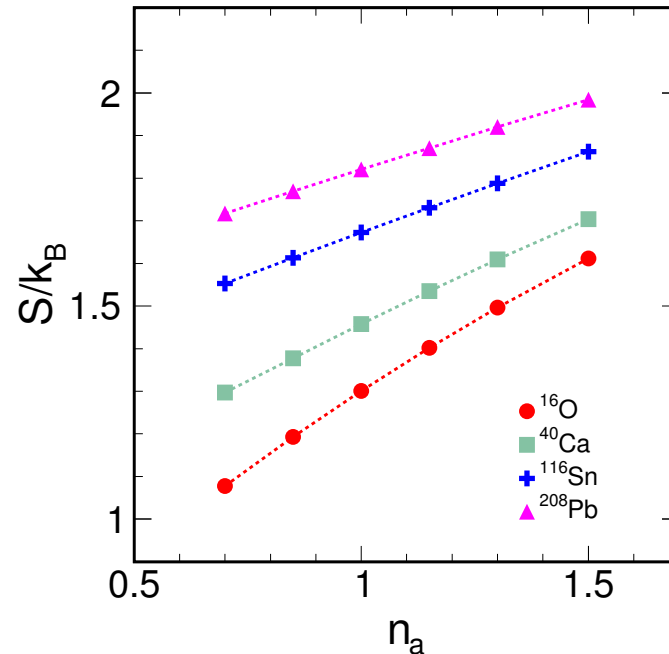


Figure 1. (color online) Information entropy varying as the diffuseness scaling parameter n_a for nuclei ^{16}O , ^{40}Ca , ^{116}Sn , and ^{208}Pb with Woods–Saxon type density distribution for nucleons.

The information entropy is observed to be a function of the neutron skin thickness in neutron-rich nuclei. This thickness is defined as the difference between the square root radii of neutrons and protons, expressed as $\delta_{np} = R_n - R_p$, where R_n and R_p are the square root radii for neutrons and protons, respectively. By fixing the parameters R_p , a_n , and a_p and varying R_n , we can examine the variable δ_{np} . With R_n varying, the density distribution changes accordingly, allowing us to calculate the entropy corresponding to each value of δ_{np} . Consequently, the information entropy can be examined as a function of neutron skin thickness in neutron-rich nuclei. As shown in Figure 2, the relationship between information entropy and neutron skin thickness is linearly positive; as the neutron skin becomes thicker, the information entropy increases in a linear mode. Among the neutron-rich nuclei studied, such as ^{48}Ca , ^{132}Sn , ^{208}Pb , and ^{218}Pb , the heavier nuclei, such as ^{218}Pb and ^{208}Pb , have higher information entropy compared to ^{132}Sn , followed by ^{48}Ca . Furthermore, all these nuclei show almost the same trend in the increase in the information entropy with respect to the neutron skin thickness. The neutron skin thickness parameter is crucial for gaining insight into the nuclear symmetry energy and the equation of state, which are fundamental aspects of nuclear physics. Information entropy provides new insights into the study of these phenomena.

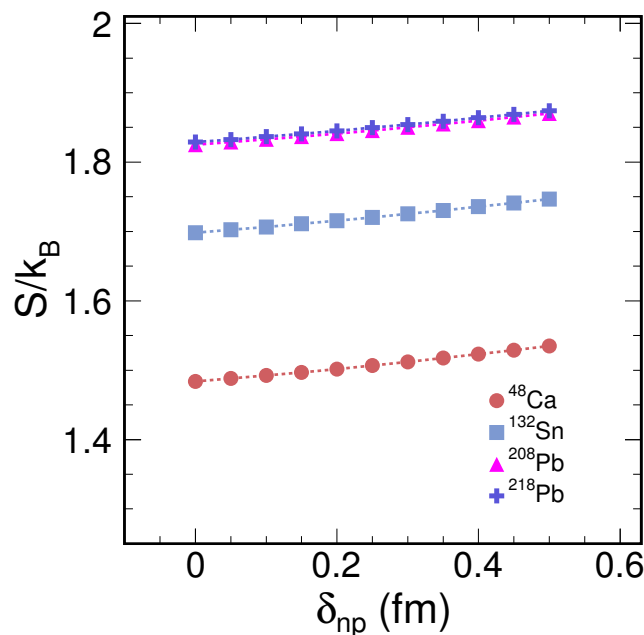


Figure 2. (color online) Information entropy varying as neutron skin thickness for nuclei ^{48}Ca , ^{132}Sn , ^{208}Pb , and ^{218}Pb with Woods–Saxon type density distribution for nucleons.

2.2. Information Entropy of The He/Li Isotope with Neutron-Rich Tail

In loosely bound nuclei, the neutron density distribution extends into an unusually long tail, known as the neutron halo phenomenon. Despite the low density that characterizes the halo, its presence significantly influences the nuclear reaction cross section and imparts special properties to these nuclei [54,55].

The analysis of proton elastic scattering cross sections for the helium isotopes ^4He , ^6He , and ^8He involves the use of four different phenomenological density distribution models [56]. These models—SF (Symmetrized Fermi), GH (Gaussian–Halo), GG (Gaussian–Gaussian), and GO (Gaussian–Oscillator)—are defined on the basis of the point-nucleon density, and each includes two free parameters. These parameters were obtained in Refs. [56–58] to reproduce an extended matter density characteristic of helium and lithium isotopes. The SF and GH parameterizations are used to model nucleon distributions in a nucleus without distinguishing between neutrons and protons. These models do not take into account the complex internal structure of many-body nuclear systems. In contrast, the GG and GO parametrizations assume a nuclear composition that includes a core and a halo, where the halo is composed entirely of neutrons, and each component has distinct spatial distributions. This approach provides a more nuanced representation of the nucleus, recognizing the spatial segregation between core nucleons and halo neutrons.

Figure 3 shows the information entropy for helium and lithium isotopes as determined by four different phenomenological density distribution models. The nucleon distribution in ^4He is optimally captured by the SF and GH parameterizations, which treat neutrons and protons equivalently and yield the lowest information entropy. Conversely, the halo nucleus ^{11}Li , which is characterized by its core-halo structure, is best described by the GH, GG, and GO models and has the highest information entropy. For ^6Li , the information entropy values are consistent across all four distribution models. Notably, the neutron-rich helium isotope has a significantly higher information entropy compared to ^4He . Models GH, GG, and GO are applied to ^6He , ^8He , ^8Li , and ^9Li . Comparing the information entropy between the neutron-rich nuclei ^6He , ^8He , ^6Li , ^8Li , and ^9Li , the values are relatively close.

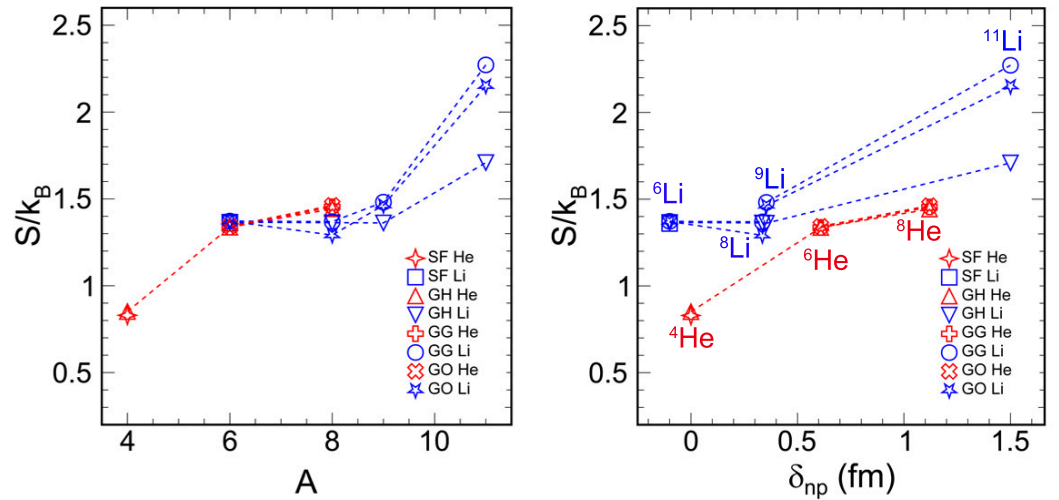


Figure 3. (color online) The information entropy for He isotope and Li isotope (left). Correlation of information entropy with neutron skin thickness for He isotope and Li isotope (right).

According to the right side of Figure 3, the information entropy is strongly correlated with the neutron skin thickness. For both lithium and helium isotopes, the information entropy increases as the neutron skin becomes thicker. Although ${}^6\text{He}$ and ${}^8\text{He}$ have larger neutron skin thicknesses, they do not exhibit significantly larger information entropies compared to ${}^6\text{Li}$, ${}^8\text{Li}$, and ${}^9\text{Li}$ due to their similar nucleon numbers.

Information entropy is a measure of uncertainty and disorder in nuclear density distributions. By evaluating the probability distribution over different points in the nucleus and their associated entropy values, we gain insight into the internal complexity of nuclear structures. Halo nuclei, such as ${}^{11}\text{Li}$, typically have higher entropy because their nuclear density is more radially dispersed.

2.3. Application of Information Entropy in Nuclear Cluster Formation

It has been suggested that atomic nuclei with tetrahedral symmetry could be found throughout the nuclear table [59]. In particular, the tetrahedral structure formed by four α particles in ${}^{16}\text{O}$ has been proposed in several studies [39,45,60–62]. The rotation–vibration spectrum of a 4α configuration with tetrahedral symmetry (denoted T_d) has been studied, and evidence for its occurrence in the lower energy levels of ${}^{16}\text{O}$ has been found through experimental excitation spectra. This symmetry-based structure has implications for several areas of physics, suggesting that atomic nuclei with tetrahedral symmetry may be of significant interest.

It was shown that the conditions for cluster formation can be traced back in part to the depth of the confining nuclear potential using the theoretical framework of energy density functionals [63,64]. The depth of the nuclear potential for a harmonic oscillator is given by

$$V_{\text{depth}} = \frac{\hbar^2 R^2}{2m b^4}, \quad (5)$$

where R is the radius of the system, m is the mass of the nucleon, \hbar is the reduced Planck constant, and b is the nucleon dispersion in the α cluster distribution. As the dimensionless ratio (of b to the typical interfermion distance r_0 , quantifying nuclear clustering) increases, the nuclear system transitions from a crystalline to a clustered and then to a quantum liquid phase. The trend curves shown on the left of Figure 4 are the depth curves of the nuclear potential versus b for three geometric situations characterized by r_α , the distance of the center of the α -cluster relative to the center of ${}^{16}\text{O}$.

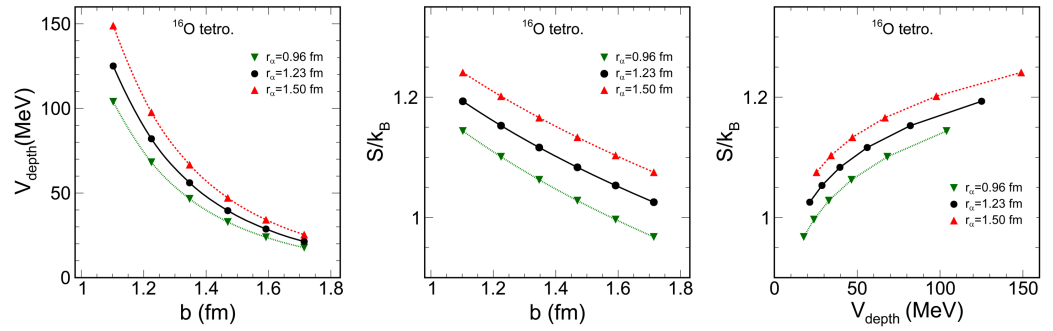


Figure 4. (color online) The nuclear potential depth curves for a harmonic oscillator in ^{16}O with tetrahedral cluster structure (**left**). The correlation of the information entropy with the cluster dispersion (**center**). The correlation of the information entropy with the depth of the nuclear potential for a harmonic oscillator (**right**).

To study the role of information entropy in ^{16}O with tetrahedral cluster structure, where the distribution of nucleons within an alpha particle based on the alpha particle model is Gaussian type [65],

$$\rho(\vec{r}) = \sum_{i=1}^4 m_i \left(\frac{\delta_i}{\pi}\right)^{3/2} e^{-\delta_i(\vec{r}-\vec{r}_i)^2}, \quad (6)$$

where $m_i = m_\alpha$ is the mass of the α cluster; $\delta_i = \delta_\alpha = 0.52$ is the nucleon distribution deviation for parameterizing the dispersion of the α cluster; $\vec{r}_i = \vec{r}_\alpha$ is the vector of the α cluster relative to the center of mass of ^{16}O . The centers of each α cluster are defined as $A = \{\beta, \frac{\pi}{2} + \arctan(\frac{\sqrt{2}}{4}), \frac{7\pi}{6}\}$; $B = \{\beta, \frac{\pi}{2} + \arctan(\frac{\sqrt{2}}{4}), \frac{11\pi}{6}\}$; and $C = \{\beta, \frac{\pi}{2} + \arctan(\frac{\sqrt{2}}{4}), \frac{\pi}{2}\}$; $D = \{\beta, 0, 0\}$, where $\beta = \frac{\sqrt{6}}{4}\lambda$, and λ is the edge length (the center distance of any two α clusters). $\beta = r_\alpha$ for the tetrahedral structure of ^{16}O .

The correlation curves of the information entropy with the cluster dispersion are shown in the middle of Figure 4 for three geometric configurations characterized by the parameter r_α . The information entropy tends to decrease monotonically as the dispersion parameter b increases. A larger r_α leads to a larger system radius, which results in a higher information entropy. The right panel of Figure 4 shows some correlation curves between information entropy and potential depth. As the potential depth gradually decreases, the information entropy also decreases.

Studies [63,64] have concluded that the formation of nuclear clusters can be partially attributed to the depth of the confining nuclear potential, and it has been observed that as the parameter b increases, the nuclear system undergoes a phase transition from a crystalline state to a clustered state and finally to a quantum liquid state. The present investigations show a significant correlation between the information entropy and the parameter b . Consequently, it could be reasonable to say that variations in the information entropy are indicative of the nuclear phase transitions.

When fitting the correlation points for a given value of r_α (i.e., a given size of the system) through a simple relation

$$S/k_B = \eta \ln \frac{V_{\text{depth}}}{V_0}, \quad (7)$$

where η and V_0 are fitting parameters, we can obtain a good prediction curve of S/k_B as a function of V_{depth} with least squares fitting accuracy χ^2 of order 10^{-5} . Equation (7) establishes a relationship between nuclear depth and information entropy, linking the microstate to randomness. A higher entropy indicates a higher degree of disorder. The depth of the nuclear potential determines the degree of confinement and energy level structure of the nucleons in the nucleus, which affects the quality, size, and shape of the

nucleus, as well as nuclear reactions. The analysis of Figure 4 suggests that for ^{16}O , which is characterized by a tetrahedral cluster structure, an increase in the depth of the nuclear potential corresponds to a greater localization of nucleons within the clusters, while higher entropy indicates increased disorder. This suggests an inherent correlation between nuclear potential depth and information entropy.

As the dispersion parameter a increases, the central density of the Woods–Saxon type ^{16}O relatively decreases, leading to a larger spread of density at a larger radius and, consequently, to an increase in information entropy (Figure 1). For ^{16}O with an alpha cluster structure, for a given alpha spacing, increasing the cluster dispersion parameter b causes the central density of the ^{16}O distribution to increase, making it more like a liquid phase. As a result, the information entropy decreases with increasing b (Figure 4), which corresponds to the situation of a lower dispersion parameter a for the Woods–Saxon type. In general, this illustrates that the more centrally distributed the nucleons are, the lower the information entropy of the system will be, and vice versa.

Information entropy is proposed as an available tool for the analysis of nuclear clustering mechanisms. By calculating the information entropy, the degree of disorder in the nuclei with cluster structures can be revealed, and their formation mechanisms can be further understood. Nuclear clustering is an important aspect of nuclear structure, and this clustering behavior is mainly observed in light nuclei, leading to unique nuclear properties that deviate from traditional mean-field models. In this case, a higher entropy value indicates a more dispersed and disordered cluster structure, while a lower entropy value implies a more centralized arrangement, like a quantum liquid phase.

3. Summary

This study investigates the role of information entropy in nuclear physics, focusing on nuclear density distributions, including halo structures and alpha clustering. Information entropy measures uncertainty and disorder, providing insight into the internal complexity of nuclear structures. There is a linear relationship between information entropy and diffusion parameters, indicating increasing uncertainty in the radial nucleon distribution with increasing diffusion. Heavier nuclei typically have higher information entropy, suggesting greater complexity in larger systems.

In addition, there is a strong correlation between information entropy and neutron skin thickness, which is an important parameter for understanding nuclear symmetry energy. The analysis of helium and lithium isotopes shows different levels of information entropy, with the halo nucleus ^{11}Li showing the highest entropy due to its widely dispersed core-halo structure. On the other hand, the most tightly bound nucleus, ^4He , has the lowest level of information entropy.

For ^{16}O , which is characterized by a tetrahedral cluster structure, the information entropy decreases as the potential depth gradually decreases. By studying the difference in information entropy in a nucleus, we can gain insight into the stability and dynamics of nuclear clusters. It underscores the value of information entropy as a key tool for revealing and exploring the diversity of nuclear structures.

Current models of nuclear density distribution, while phenomenological rather than based on microscopic quantum mechanics, effectively capture the approximate features of nucleon distribution in atomic nuclei. Information entropy offers a novel perspective by quantifying the diversity of nuclear structures, thereby improving our understanding of nuclear systems. However, these models are limited in that they do not fully capture the subtleties of quantum effects at the microscopic level. In future studies, we aim to further validate the current concepts and results by incorporating microscopic density distributions of atomic nuclei.

Author Contributions: Conceptualization, Y.G. Ma and W.H. Ma; methodology, Y.G. Ma and W.H. Ma; software, W.H. Ma; validation, Y.G. Ma and W.H. Ma; formal analysis, Y.G. Ma and W.H. Ma; investigation, Y.G. Ma and W.H. Ma; resources, Y.G. Ma and W.H. Ma; data curation, W.H. Ma; writing—original draft preparation, W.H. Ma; writing—review and editing, Y.G. Ma; visualization,

W.H. Ma; supervision, Y.G. Ma; project administration, Y.G. Ma; funding acquisition, Y.G. Ma and W.H. Ma. All authors have read and agreed to the published version of the manuscript.

Funding: This work is supported by the Natural Science Foundation of Shanghai with Grants No. 23JC1400200, the National Natural Science Foundation of China with Grants No. 11905036, 12147101 and 11890710, the National Key R&D Program from the Ministry of Science and Technology of China (2022YFA1604900), and the STCSM under Grant No. 23590780100.

Data Availability Statement: No new data were created or analyzed in this study. Data sharing is not applicable to this article.

Acknowledgments: We have no additional acknowledgments to make.

Conflicts of Interest: The authors declare no conflicts of interest.

References

1. Shannon, C.E. A mathematical theory of communication. *Bell Syst. Tech. J.* **1948**, *27*, 379–423. <https://doi.org/10.1002/j.1538-7305.1948.tb01338.x>.
2. Ma, Y.G. Application of information theory in nuclear liquid gas phase transition. *Phys. Rev. Lett.* **1999**, *83*, 3617. <https://doi.org/10.1103/PhysRevLett.83.3617>.
3. Ma, Y.G.; Natowitz, J.B.; Wada, R.; Hagel, K.; Wang, J.; Keutgen, T.; Majka, Z.; Murray, M.; Qin, L.; Smith, P.; Alfaro, R. Critical behavior in light nuclear systems: Experimental aspects. *Phys. Rev. C* **2005**, *71*, 054606. <https://doi.org/10.1103/PhysRevC.71.054606>.
4. Ma, Y.G.; Pang, L.G.; Wang, R.; Zhou, K. Phase transition study meets machine learning. *Chin. Phys. Lett.* **2023**, *40*, 122101. <https://doi.org/10.1088/0256-307X/40/12/122101>.
5. Denbigh, K.G.; Denbigh, J.S. *Entropy in Relation to Uncomplete Knowledge*; Cambridge University: Cambridge, UK, 1995.
6. Longair, M.S. *Theoretical Concepts in Physics*; University Press: Oxford, UK, 1984; Chapter 10: Kinetic theory and the origin of statistical mechanics; ISBN 0521821266.
7. Moustakidis, C.C.; Massen, S.E.; Panos, C.P.; Grypeos, M.E. and Antonov, A.N. Evaluation of cluster expansions and correlated one-body properties of nuclei. *Phys. Rev. C* **2001**, *64*, 014314. <https://doi.org/10.1103/PhysRevC.64.014314>
8. Massen, S.E. Application of information entropy to nuclei. *Phys. Rev. C* **2003**, *67*, 014314. <https://doi.org/10.1103/PhysRevC.67.014314>.
9. Csernai, L.; Kapusta, J.I. Entropy and cluster production in nuclear collisions. *Phys. Rep.* **1986**, *131*, 223. [https://doi.org/10.1016/0370-1573\(86\)90031-1](https://doi.org/10.1016/0370-1573(86)90031-1).
10. Ma, C.W.; Ma, Y.G. Shannon information entropy in heavy-ion collisions. *Progr. Part. Nucl. Phys.* **2018**, *99*, 120. <https://doi.org/10.1016/j.pnpnp.2018.01.002>.
11. Cao, Z.; Hwa, R.C. Chaotic behavior of particle production in branching processes. *Phys. Rev. D* **1996**, *53*, 6608. <https://doi.org/10.1103/PhysRevD.53.6608>.
12. Ma, C.W.; Wei, H.L.; Wang, S.S.; Ma, Y.G.; Wada, R.; Zhang, Y.L. Isobaric yield ratio difference and Shannon information entropy. *Phys. Lett. B* **2015**, *742*, 19. <https://doi.org/10.1016/j.physletb.2015.01.015>
13. Xu, J.; Ko, C.M. Chemical freeze-out in relativistic heavy-ion collisions. *Phys. Lett. B* **2017**, *772*, 290. <https://doi.org/10.1016/j.physletb.2017.06.061>.
14. Csernai, L.; Spinnangr, S.; Velle, S. Quantitative assessment of increasing complexity. *Phys. A Stat. Mech. Appl.* **2017**, *473*, 363. <https://doi.org/10.1016/j.physa.2016.12.091>.
15. Lichtenberg, D.B.; Namgung, W.; Predazzi, E.; Wills, J.G. Baryon Masses in a Relativistic Quark-Diquark Model. *Phys. Rev. Lett.* **1982**, *48*, 1653. <https://doi.org/10.1103/PhysRevLett.48.1653>.
16. Ma, C.W.; Liu, Y.P.; Wei, H.L.; Pu, J.; Cheng, K.X.; Wang, Y.T. Determination of neutron-skin thickness using configurational information entropy. *Nucl. Sci. Tech.* **2022**, *33*, 6. <https://doi.org/10.1007/s41365-022-00997-0>.
17. Wei, H.L.; Zhu, X.; Yuan, C. Configurational information entropy analysis of fragment mass cross distributions to determine the neutron skin thickness of projectile nuclei. *Nucl. Sci. Tech.* **2022**, *33*, 111. <https://doi.org/10.1007/s41365-022-01096-w>.
18. Biales, A.; Peshanshi, R. Moments of rapidity distributions as a measure of short-range fluctuations in high-energy collisions. *Nucl. Phys. B* **1986**, *273*, 703–718. [https://doi.org/10.1016/0550-3213\(86\)90386-X](https://doi.org/10.1016/0550-3213(86)90386-X).
19. Li, F.; Chen, G. The evolution of information entropy components in relativistic heavy-ion collisions. *Eur. Phys. J. A* **2020**, *56*, 167. <https://doi.org/10.1140/epja/s10050-020-00169-x>.
20. Pu, J.; Yu, Y.B.; Cheng, K.X.; Wang, Y.T.; Guo, Y.F.; Ma, C.W. Exploring critical fluctuation phenomenon according to net-proton multiplicity information entropy in AMPT model. *Phys. Lett. B* **2023**, *841*, 137909. <https://doi.org/10.1016/j.physletb.2023.137909>.
21. Deng, X.G.; Ma, Y.G. Information entropy for central 197Au+197Au collisions in the UrQMD model. *arXiv*, **2024**, arXiv:2404.03424. <https://doi.org/10.48550/arXiv.2404.03424>.
22. Tanihata, I.; Hamagaki, H.; Hashimoto, O.; Shida, Y.; Yoshikawa, N.; Sugimoto, K.; Yamakawa, O.; Kobayashi, T.; Takahashi, N. Measurements of Interaction Cross Sections and Nuclear Radii in the Light p-Shell Region. *Phys. Rev. Lett.* **1985**, *55*, 2676. <https://doi.org/10.1103/PhysRevLett.55.2676>.

23. Xu, S.Z.; Zhang, S.S.; Jiang, X.Q.; Scott, S.M. The complex momentum representation approach and its application to low-lying resonances in 17 O and 29 F. *Nucl. Sci. Tech.* **2023**, *34*, 5. <https://doi.org/10.1007/s41365-022-01159-y>.
24. Bagchi, S.; Kanungo, R.; Tanaka, Y.K.; Geissel, H.; Doornenbal, P.; Horiuchi, W.; Hagen, G.; Suzuki, T.; Tsunoda, N.; Ahn, D.S.; Baba, H. Two-Neutron Halo is Unveiled in 29F. *Phys. Rev. Lett.* **2020**, *124*, 222504. <https://doi.org/10.1103/PhysRevLett.124.222504>.
25. Fang, D.Q. Neutron skin thickness and its effects in nuclear reactions. *Nucl. Tech.* **2023**, *46*, 080016. <https://doi.org/10.11889/j.0253-3219.2023.hjs.46.080016>.
26. Zhang, S.; Zhang, Y.F.; Xu, F.R. First-principles Gamow shell model study of nuclei in the drip line region. *Nucl. Tech.* **2023**, *46*, 080012. <https://doi.org/10.11889/j.0253-3219.2023.hjs.46.080012>.
27. Ma, Y.G.; Zhang, S.; Influence of Nuclear Structure in Relativistic Heavy-Ion Collisions. In *Handbook of Nuclear Physics*; Springer: Singapore, 2023. https://doi.org/10.1007/978-981-15-8818-1_5-1.
28. Chen, J.; Dong, X.; Ma, Y.G.; Xu, Z. Measurements of the lightest hypernucleus (3KH): Progress and perspective. *Sci. Bull.* **2023**, *68*, 3252–3260. <https://doi.org/10.1016/j.scib.2023.11.045>.
29. Zhou, L.; Fang, D.Q.; Wang, S.M.; Hua, H. Structure and 2p decay mechanism of 18 Mg. *Nucl. Sci. Tech.* **2024**, *35*, 107. <https://doi.org/10.1007/s41365-024-01479-1>.
30. Su, Y.; Li, Z.Y.; Liu, L.L.; Dong, G.X.; Wang, X.B.; Chen, Y.J. Sensitivity impacts owing to the variations in the type of zero-range pairing forces on the fission properties using the density functional theory. *Nucl. Sci. Tech.* **2024**, *35*, 62. <https://doi.org/10.1007/s41365-024-01422-4>.
31. Yan, T.Z.; Li, S. Isotopic dependence of the yield ratios of light fragments from different projectiles and their unified neutron skin thicknesses. *Nucl. Sci. Tech.* **2024**, *35*, 65. <https://doi.org/10.1007/s41365-024-01425-1>.
32. Zheng, Z.Y.; Chen, S.W.; Liu, Q. The breaking of spin symmetry in the single-particle resonances in deformed nuclei. *Nucl. Sci. Tech.* **2024**, *35*, 66. <https://doi.org/10.1007/s41365-024-01426-0>.
33. Geng, K.P.; Du, P.X.; Li, J.; Fang, D.L. Calculation of microscopic nuclear level densities based on covariant density functional theory. *Nucl. Sci. Tech.* **2023**, *34*, 141. <https://doi.org/10.1007/s41365-023-01298-w>.
34. An, R.; Sun, S.; Cao, L.G.; Zhang, F.S.; Constraining nuclear symmetry energy with the charge radii of mirror-pair nuclei. *Nucl. Sci. Tech.* **2023**, *34*, 119. <https://doi.org/10.1007/s41365-023-01269-1>.
35. Huo, E.B.; Li, K.R.; Qu, X.Y.; Zhang, Y.; Sun, T.T. Continuum Skyrme Hartree-Fock-Bogoliubov theory with Green's function method for neutron-rich Ca, Ni, Zr, and Sn isotopes. *Nucl. Sci. Tech.* **2023**, *34*, 105. <https://doi.org/10.1007/s41365-023-01261-9>.
36. von Oertzen, W.; Freer, M.; Kanada-En'yo, Y. Nuclear clusters and nuclear molecules. *Phys. Rep.* **2006**, *432*, 43. <https://doi.org/10.1016/j.physrep.2006.07.001>.
37. Ma, W.H.; Patel, D.; Yang, Y.Y.; Wang, J.S.; Kanada-En'yo, Y.; Chen, R.F.; Lubian, J.; Ye, Y.L.; Yang, Z.H.; Ren, Z.Z.; Mukherjee, S. Observation of He 6+ t cluster states in Li 9. *Phys. Rev. C* **2021**, *103*, L061302. <https://link.aps.org/doi/10.1103/PhysRevC.103.L061302>.
38. Horiuchi, H. Outlook and future perspectives. In *Journal of Physics: Conference Series*; IOP Publishing: Bristol, UK, 2008; Volume 111, p. 012054. <https://doi.org/10.1088/1742-6596/111/1/012054>
39. He, W.B.; Ma, Y.G.; Cao, X.G.; Cai, X.Z.; Zhang, G.Q. Giant Dipole Resonance as a Fingerprint of α Clustering Configurations in C 12 and O 16. *Phys. Rev. Lett.* **2014**, *113*, 032506. <https://doi.org/10.1103/PhysRevLett.113.032506>.
40. Zhou, B.; Funaki, Y.; Horiuchi, H.; Ma, Y.G.; Röpke, G.; Schuck, P.; Tohsaki, A.; Yamada, T. The 5 α condensate state in 20Ne. *Nat. Commun.* **2023**, *14*, 8206. <https://doi.org/10.1038/s41467-023-43816-9>.
41. Wang, Y.Z.; Zhang, S.; Ma, Y.G. System dependence of away-side broadening and α -clustering light nuclei structure effect in dihadron azimuthal correlations. *Phys. Lett. B* **2022**, *831*, 137198. <https://doi.org/10.1016/j.physletb.2022.137198>.
42. Wang, S.S.; Ma, Y.G.; He, W.B.; Fang, D.Q.; Cao, X.G. Influences of α -clustering configurations on the giant dipole resonance in hot compound systems. *Phys. Rev. C* **2023**, *108*, 014609 <https://doi.org/10.1103/PhysRevC.108.014609>.
43. Cao, Y.T.; Deng, X.G.; Ma, Y.G. Effect of initial-state geometric configurations on the nuclear liquid-gas phase transition. *Phys. Rev. C* **2023**, *108*, 024610. <https://doi.org/10.1103/PhysRevC.108.024610>.
44. Cao, R.X.; Zhang, S.; Ma, Y.G. Effects of the α -cluster structure and the intrinsic momentum component of nuclei on the longitudinal asymmetry in relativistic heavy-ion collisions. *Phys. Rev. C* **2023**, *108*, 064906. <https://doi.org/10.1103/PhysRevC.108.064906>.
45. Ma, Y.G. Effects of α -clustering structure on nuclear reaction and relativistic heavy-ion collisions. *Nucl. Tech.* **2023**, *46*, 080001. <https://doi.org/10.11889/j.0253-3219.2023.hjs.46.080001>.
46. Zhang, Y.X.; Zhang, S.; Ma, Y.G. Signatures of an α + core structure in $^{44}\text{Ti} + ^{44}\text{Ti}$ collisions at $\sqrt{s_{\text{NN}}} = 5.02$ TeV by a multiphase transport model. *Euro. Phys. J. A* **2024**, *60*, 73. <https://doi.org/10.1140/epja/s10050-024-01290-x>.
47. Ozawa, A.; Matter Radii and Density Distributions. In *Handbook of Nuclear Physics*; Springer: Singapore, 2023. https://doi.org/10.1007/978-981-15-8818-1_40-1.
48. Ding, M.Q.; Fang, D.Q.; Ma, Y.G. Effects of neutron-skin thickness on light-particle production. *Phys. Rev. C* **2024**, *109*, 024616. <https://doi.org/10.1103/PhysRevC.109.024616>.
49. Thomas, M.T.C.A.J.; Joy, A.T. *Elements of Information Theory, Second Edition*; John Wiley & Sons, Inc.: Hoboken, NJ, USA, 2006.
50. Woods, R.D.; Saxon, D.S. Diffuse Surface Optical Model for Nucleon-Nuclei Scattering. *Phys. Rev.* **1954**, *95*, 577 <https://doi.org/10.1103/PhysRev.95.577>.

51. Vries, H.D.; Jager, C.W.D.; Vries, C.D. Nuclear charge-density-distribution parameters from elastic electron scattering. *At. Data Nucl. Data Tables* **1987**, *36*, 495–536. [https://doi.org/10.1016/0092-640X\(87\)90013-1](https://doi.org/10.1016/0092-640X(87)90013-1).
52. Chamon, L.C.; Carlson, B.V.; Gasques, L.R.; Pereira, D.; De Conti, C.; Alvarez, M.A.G.; Hussein, M.S.; Ribeiro, M.C.; Rossi, E.S., Jr.; Silva, C.P. *Phys. Rev. C* **2002**, *66*, 014610. <https://doi.org/10.1103/PhysRevC.66.014610>.
53. Shou, Q.Y.; Ma, Y.G.; Sorensen, P.; Tang, A.H.; Videbæk, F.; Wang, H. Parameterization of deformed nuclei for Glauber modeling in relativistic heavy ion collisions. *Phys. Lett. B* **2015**, *749*, 215. .
54. Tanihata, I. Neutron halo nuclei. *J. Phys. G: Nucl. Part. Phys.* **1996**, *22*, 157. <https://doi.org/10.1088/0954-3899/22/2/004>.
55. Parker, M.C.; Jeynes, C.; Catford, W.N. Halo properties in helium nuclei from the perspective of geometrical thermodynamics. *Ann. Der Phys. Park.* **2022**, *534*, 2100278. <https://doi.org/10.1002/andp.202100278>.
56. Alkhozov, G.D.; Dobrovolsky, A.V.; Egelhof, P.; Geissel, H.; Irnich, H.; Khanzadeev, A.V.; Korolev, G.A.; Lobodenko, A.A.; Münzenberg, G.; Mutterer, M.; Neumaier, S.R. Nuclear matter distributions in the ${}^6\text{He}$ and ${}^8\text{He}$ nuclei from differential cross sections for small-angle proton elastic scattering at intermediate energy. *Nucl. Phys. A* **2002**, *712*, 269–299. [https://doi.org/10.1016/S0375-9474\(02\)01273-3](https://doi.org/10.1016/S0375-9474(02)01273-3).
57. Dobrovolsky, A.V.; Alkhozov, G.D.; Andronenko, M.N.; Bauchet, A.; Egelhof, P.; Fritz, S.; Geissel, H.; Gross, C.; Khanzadeev, A.V.; Korolev, G.A.; Kraus, G. Study of the nuclear matter distribution in neutron-rich Li isotopes. *Nucl. Phys. A* **2006**, *766*, 1–24. <https://doi.org/10.1016/j.nuclphysa.2005.11.016>.
58. Moriguchi, T.; Ozawa, A.; Ishimoto, S.; Abe, Y.; Fukuda, M.; Hachiuma, I.; Ishibashi, Y.; Ito, Y.; Kuboki, T.; Lantz, M.; Nagae, D. Density distributions of ${}^{11}\text{Li}$ deduced from reaction cross-section measurements. *Phys. Rev. C* **2013**, *88*, 024610. <https://doi.org/10.1103/PhysRevC.88.024610>.
59. Dudek, J.; Gozdz, A.; Schunck, N.; Miskiewicz, M. Nuclear tetrahedral symmetry: possibly present throughout the periodic table. *Phys. Rev. Lett.* **2002**, *88*, 252502. <https://doi.org/10.1103/PhysRevLett.88.252502>.
60. Bijker, R.; Iachello, F. Evidence for Tetrahedral Symmetry in O 16. *Phys. Rev. Lett.* **2014**, *112*, 152501. <https://doi.org/10.1103/PhysRevLett.112.152501>.
61. Ding, C.; Pang, L.G.; Zhang, S.; Ma, Y.G. Signals of α clusters in $16\text{O}+16\text{O}$ collisions at the LHC from relativistic hydrodynamic simulations. *Chin. Phys. C* **2023**, *47*, 024105. <https://doi.org/10.1088/1674-1137/ac9fb8>.
62. Ma, Y. G.; Zhang, S. α -clustering effects in relativistic heavy-ion collisions. *Sci. Sin.-Phys. Mech. Astron.* **2024**, *54*, 292004. <https://doi.org/10.1360/SSPMA-2024-0013>. (in Chinese)
63. Ebran, J.P.; Khan, E.; Nikšić, T.; Vretenar, D. How atomic nuclei cluster. *Nature* **2012**, *487*, 341–344. <https://doi.org/10.1038/nature11246>.
64. Ebran, J.P.; Khan, E.; Nikšić, T.; Vretenar, D. Localization and clustering in atomic nuclei. *J. Phys. G: Nucl. Part. Phys.* **2017**, *44*, 103001. <https://doi.org/10.1088/1361-6471/aa809b>.
65. Bijker, R. The algebraic cluster model: three-body clusters. *Ann. Phys.* **2002**, *298*, 334–360. <https://doi.org/10.1006/aphy.2002.6255>

Disclaimer/Publisher’s Note: The statements, opinions and data contained in all publications are solely those of the individual author(s) and contributor(s) and not of MDPI and/or the editor(s). MDPI and/or the editor(s) disclaim responsibility for any injury to people or property resulting from any ideas, methods, instructions or products referred to in the content.